Monatsh Chem 139, 1169–1174 (2008)
DOI 10.1007/s00706-008-0911-7
Printed in The Netherlands

Monatshefte für Chemie
Chemical Monthly

Formation of sodium 6-hydroxy-2-naphthoate in the *Kolbe-Schmitt* reaction

Svetlana Marković[1], Igor Đurović[1], Zoran Marković[2]

[1] Faculty of Science, University of Kragujevac, Kragujevac, Serbia
[2] Faculty of Agronomy, University of Kragujevac, Čačak, Serbia

Received 14 February 2008; Accepted 16 February 2008; Published online 11 April 2008

Abstract This work is an extension of our investigation of the mechanism of the *Kolbe-Schmitt* reaction of sodium 2-naphthoxide. The carboxylation reaction of sodium 2-naphthoxide in the position 6 is examined by means of the *B3LYP*/LANL2DZ method. After the initial formation of sodium 2-naphthoxide-CO_2 complex, the carbon of the CO_2 moiety performs an electrophilic attack on the naphthalene ring in position 8. Further transformations lead to the formation of sodium 6-hydroxy-2-naphthoate. Our findings are in good agreement with the experimental results on the carboxylation reaction of sodium 2-naphthoxide.

Keywords *Kolbe-Schmitt* reaction; Sodium 2-naphthoxide; Sodium 6-hydroxy-2-naphthoate; Reaction mechanism; *B3LYP*/LANL2DZ.

Introduction

The *Kolbe-Schmitt* reaction is an important source of numerous industrial products. Although the reaction has been known for almost 150 years [1–9], it is a subject of novel experimental and theoretical investigations [10–20]. The details on carboxylation reactions of alkali metal phenoxides [7–19] and early investigations of the *Kolbe-Schmitt* reaction of sodium 2-naphthoxide (**1**) [4–8] can be found in cited literature, and the references given therein. Here we refer to the novel investigations concerning the carboxylation reaction of **1**.

The work of *Rahim*, *Matsui*, and *Kosugi* has provided valuable information on the carboxylations of various alkali and alkaline earth metal 2-naphthoxides [11]. It has been shown that **1** needed to be heated above 200°C to produce a mixture of 2-hydroxy-1-naphthoic acid and 3- and 6-hydroxy-2-naphthoic acids. For example, in an experiment performed at 5 MPa and 230°C, the yields of 2-hydroxy-1-naphthoic, 3-hydroxy-2-naphthoic, and 6-hydroxy-2-naphthoic acids amounted to 14.5, 71.5, and 2.5%. In spite of the low yield of 6-hydroxy-2-naphthoic acid, it is an important product of the *Kolbe-Schmitt* reaction, since a copolymerization of 4-hydroxybenzoic and 6-hydroxy-2-naphthoic acids gives an engineering plastic of high quality [21].

In a recent study [20], the mechanism of the carboxylation reaction of **1** in the positions 1 and 3 has been investigated by means of the *B3LYP*/LANL2DZ method. It has been shown that after the initial formation of the sodium 2-naphthoxide-CO_2 complex, the carbon of the CO_2 moiety performed an electrophilic attack on the naphthalene ring in position 1. Further transformations led to the formation of sodium 2-hydroxy-1-naphthoate, whereas sodium 3-hydroxy-2-naphthoate was formed by a 1,3-rearrangement of the CO_2Na group. In Ref. [20] the formation of sodium 6-hydroxy-2-naphthoate has not been considered. The aim of this work is to fill this gap. Thus, we investigate the carboxylation reaction of **1** in position 6.

Correspondence: Svetlana Marković, Faculty of Science, University of Kragujevac, 34000 Kragujevac, Serbia. E-mail: mark@kg.ac.yu

Results and discussion

Before we present our results we need to fix the notation used in this work. Formulae numbers **2**, **4**, **6**, **8**, and **10** represent intermediates; **3**, **5**, **7**, **9**, and **11** stand for transition states; **12** denotes a free radical, whereas **13** represents sodium 6-hydroxy-2-naphthoate (Fig. 1).

Our calculations reveal that the carboxylation reaction in position 6 of **1** (*i.e.*, the formation of **13**) proceeds *via* five intermediates and five transition states. The scheme of the mechanism and energetic diagram of the reaction are presented in Fig. 1. The values of the total energies, enthalpies, and free energies of all relevant species are given in Table 1. The optimized geometries of all transition states in the reaction are presented in Fig. 2, whereas the bond lengths of all intermediates and transition states are given in Table 2. The values of the natural bond orbital charges for all heavy atoms of the intermediates are presented in Table 3.

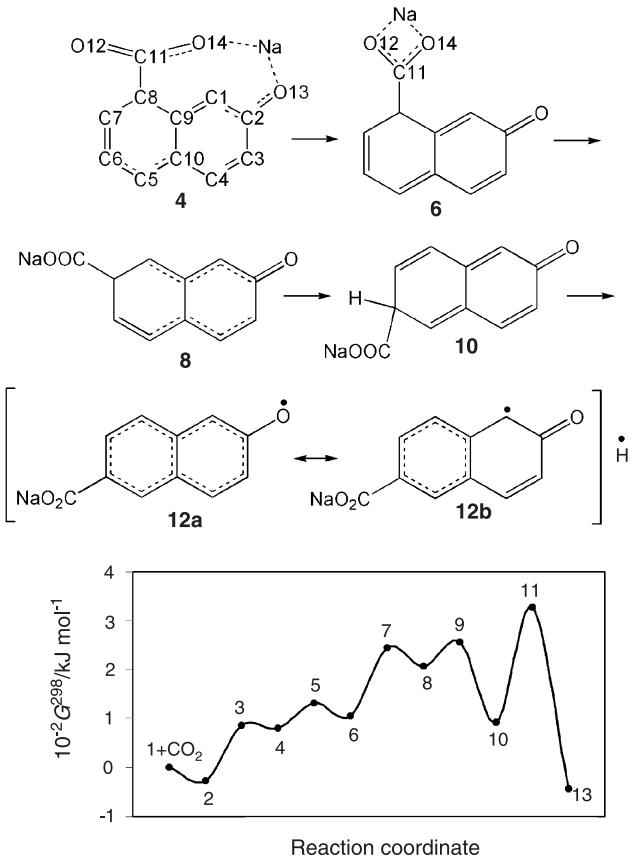

Fig. 1 Mechanistic scheme and energy profile for the carboxylation reaction of sodium 2-naphthoxide in position 6. $\mathbf{1} + CO_2$ – reactands; **2**, **4**, **6**, **8**, **10** – intermediates; **3**, **5**, **7**, **9**, **11** – transition states; **12** – free radical; **13** – product

Table 1 Total energies (E), enthalpies (H^{298}), and free energies (G^{298}) for all participants in the investigated reaction. The values for $\mathbf{1} + CO_2$ and **2** are given in Ref. [20]

Species	$-E$/a.u.	$-H^{298}$/a.u.	$-G^{298}$/a.u.
3	649.0641	649.051112	649.102758
4	649.065583	649.052115	649.104725
5	649.047688	649.035011	649.085801
6	649.054701	649.041145	649.095821
7	649.002482	648.989084	649.042523
8	649.015899	649.002235	649.05685
9	648.998015	648.984655	649.037886
10	649.059649	649.046165	649.100521
11	648.970076	648.956549	649.010809
12	648.489701	648.476685	648.529776
13	649.112391	649.099127	649.151822

Our investigation shows that the reaction of **1** with CO_2 begins with the formation of the intermediate sodium 2-naphthoxide-carbon dioxide complex **2** (diagram in Fig. 1). The formation and properties of **2** have been described in Ref. [20]. Here we point out that in **2** C11 bears strong positive charge, whereas C1, C3, C6, C7, and C8 are partially negatively charged. In addition, the greatest contribution to the HOMO comes from the C1, C4, C5, C6, and C8 atoms. On the basis of the natural bond orbital charge and HOMO analyses of **2** one can assume that the strongly electrophilic C11 can perform an attack on a partially negatively charged carbon atom with a great contribution to the HOMO, *i.e.*, on C1, C6, or C8. A reaction path in position 1 has been examined [20]. Our calculations show that an attack of C11 on C8 proceeds *via* the transition state **3** with the formation of the intermediate **4** where sodium is chelated with the O13 and O14 atoms (Table 1 and Figs. 1 and 2). A significant feature of the structures **3** and **4** is that O13, Na, O14, and C11 form a bridge between the C2 and C8 atoms. As a consequence, the C2 and C8 atoms of **3** and **4** lie out of the plane of the naphthalene ring by around 7 and 5°. It is worth pointing out that an electrophilic attack of C11 on C6 is also examined, but a reaction path is not found. This is apparently due to the short ionic radius of sodium, so that possible geometries analogous to **3** and **4** (where O13, Na, O14, and C11 form a bridge between the C2 and C6 atoms) would require significant deformations of the naphthalene ring.

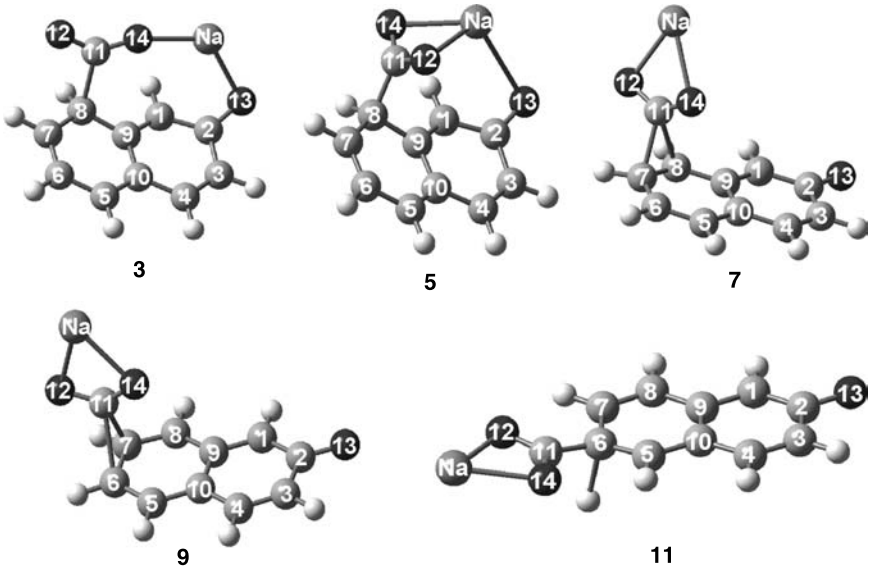

Fig. 2 Optimized geometries of all transition states

Table 2 Selected distances between atoms for all intermediates, transition states, and the free radical[a]

Dist./nm	3	4	5	6	7	8	9	10	11	12
C5–C6	0.143	0.143	0.145	0.145	0.140	0.137	0.140	0.150	0.142	0.140
C6–C7	0.139	0.138	0.137	0.136	0.143	0.150	0.147	0.151	0.145	0.143
C7–C8	0.146	0.147	0.149	0.151	0.145	0.149	0.141	0.136	0.138	0.139
C8–C9	0.147	0.148	0.153	0.154	0.143	0.140	0.143	0.147	0.144	0.144
C9–C10	0.145	0.146	0.146	0.147	0.147	0.148	0.148	0.148	0.144	0.145
O12–Na	0.450	0.447	0.244	0.228	0.234	0.228	0.234	0.227	0.226	0.226
O13–Na	0.232	0.235	0.317	0.630	0.723	0.940	0.829	0.994	1.046	1.045
O14–Na	0.218	0.216	0.235	0.226	0.232	0.229	0.230	0.227	0.226	0.226
C8–C11	0.190	0.178	0.160	0.156	0.213	0.254	0.273	0.371	0.382	0.381
C7–C11	0.270	0.263	0.260	0.253	0.192	0.157	0.190	0.255	0.260	0.253
C6–C11	0.373	0.369	0.361	0.365	0.278	0.258	0.214	0.156	0.152	0.150

[a] Some bond lengths do not undergo significant changes during the reaction. The C2–O13, C11–O12, and C11–O14 bond lengths amount to around 0.13 nm, whereas the C1–C2, C1–C9, C2–C3, C3–C4, C4–C10, and C5–C10 bond lengths lie in the interval of 0.14–0.15 nm

The natural bond orbital analysis of **4** reveals a weak single C8–C11 bond whose hybrid composition is $0.76(sp^{5.31})_{C8} + 0.65(sp^{2.84})_{C11}$. The predominant p character with little s mixing in hybridization on C8 is in agreement with the C8–C11 bond length of 0.1781 nm. A consequence of the strong p character on C8 is that the C7–C8 and C8–C9 bonds are elongated (Table 2) in comparison to intermediate **2** [20].

In **4** the positively charged sodium is attracted by the negatively charged O12 and O14 (Table 3). This attraction leads to the formation of the intermediate **6** *via* the transition state **5** (Table 1 and Figs. 1 and 2). In **5** sodium is chelated with three oxygen atoms, so that the bridge over the naphthalene ring still exists, and the carbonyl group significantly deviates from the plane of the naphthalene ring (by about 15°). In **6** the link between the Na and O13 atoms is broken, and sodium is now chelated with the O12 and O14 atoms (Fig. 1). Consequently, the planar structure of the naphthalene ring is reestablished. The C8–C11 bond is completely formed, and its hybrid composition is $0.73(sp^{3.23})_{C8} + 0.68(sp^{1.74})_{C11}$. A significant reduction of the p character in hybridization on C8 in comparison to **4** is observed (Table 2).

The vicinity of electron rich double C6–C7 bond in **6** indicates that the CO_2Na group can rearrange

Table 3 Natural bond orbital charges on heavy atoms in intermediates and the free radical

Atom	**4**	**6**	**8**	**10**	**12**
C1	−0.322	−0.262	−0.258	−0.258	−0.156
C2	0.436	0.461	0.386	0.465	0.382
C3	−0.263	−0.250	−0.153	−0.252	−0.238
C4	−0.171	−0.182	−0.233	0.172	−0.185
C5	−0.106	−0.131	−0.220	−0.086	−0.164
C6	−0.266	−0.251	−0.156	−0.388	−0.112
C7	−0.078	−0.097	−0.412	−0.151	−0.187
C8	−0.398	−0.381	−0.013	−0.221	−0.172
C9	0.022	0.009	−0.101	−0.025	−0.073
C10	−0.092	−0.073	−0.009	−0.089	−0.039
O13	−0.769	−0.602	−0.706	−0.597	−0.522
Na	0.953	0.937	0.943	0.937	0.936
C11	0.885	0.829	0.837	0.835	0.794
O12	−0.646	−0.820	−0.821	−0.827	−0.832
O14	−0.824	−0.830	−0.809	−0.830	−0.832

from C8 to the negatively charged C6 (Table 3), and then undergo further transformations. Our investigation shows that a migration of the CO_2Na group occurs *via* two successive steps. In the first step the CO_2Na group rearranges from C8 to C7, thus forming **8** *via* the transition state **7**. In the second step of the migration the CO_2Na group rearranges from C7 to C6 forming the intermediate **10** *via* transition state **9** (Table 1 and Figs. 1 and 2).

In **7** the C8–C11 bond is being broken, whereas the C7–C11 bond is being formed (Fig. 2 and Table 2). The C8, C11, and C7 atoms form a three-membered ring. The natural bond orbital analysis of **7** shows that C6, C7, and C11 form a 3-center hyperbond whose occupancy is 2.93, and the contributions of the C6–C7 and C7–C11 bonds amount to 40.5 and 59.5%. This hyperbond, as well as the C7–C11 and C8–C11 distances, indicate that **7** is a late transition state. In **8** (Fig. 1 and Table 2) the C8–C11 bond is completely broken, whereas the C7–C11 bond is completely formed with a hybrid composition of $0.74(sp^{3.21})_{C7} + 0.68(sp^{1.82})_{C11}$. In comparison to **6**, where C7 is sp^2 hybridized, there is an increase of the p character on C7 in **8**. As a consequence, C6–C7 is now a single bond. On the other hand, the contribution of the s orbital in hybridization on C5 and C6 is increased, so that C5–C6 becomes a double bond.

In **9** the C7–C11 bond is being broken, whereas the C6–C11 bond is being formed (Fig. 2 and Table 2). Here, a three-membered ring is formed by the C6, C7, and C11 atoms. In **10** the C7–C11 bond is completely broken (Fig. 1 and Table 2), and the contribution of the p orbital in sp hybridization on C7 is reduced (about sp^2). The C6–C11 bond is completely formed, and its hybrid composition is $0.73(sp^{3.17})_{C6} + 0.68(sp^{1.72})_{C11}$. A consequence of the predominant p character on C6 is that the C5–C6 and C6–C7 bonds are elongated in comparison to **8**. This particularly refers to C5–C6, which is now a single bond.

In **6**, **8**, and **10** the aromatic structure on the C8, C7, and C6 atoms is perturbated, and, certainly, the CO_2Na group and the corresponding hydrogen atoms lie out of the plane of the ring. For example, the deviations of the CO_2Na group and hydrogen on C6 in **10** amount to approximately 22°.

A possibility of formation of free radicals in the mechanism of the *Kolbe-Schmitt* reaction has not been considered until recently [19]. Taking into account the high temperatures at which the reaction is performed, it is reasonable to expect that free radicals are likely to be formed. For this reason, homolytic cleavage of the C6–H bond of **10** is examined. Our investigation reveals a transformation of **10** to **13** *via* transition state **11**, with an expectedly high activation energy (Fig. 1 and Table 1).

In **11** the C6–H bond is being broken (Fig. 2 and Table 2). As a consequence, the CO_2M group slightly deviates from the plane of the naphthalene ring (about 7°). On the other hand, a deviation of C6 from the planarity is observed (about 4°).

Figure 1 shows that **11** can transform to either **10** or **13**. In the text that follows we consider which direction for the transformation of **11** is more favorable. For this purpose, the hydrogen atom is abstracted from **11**, and the so-obtained free radical **12** is optimized (Fig. 1 and Table 1).

The natural bond orbital analysis of **12** shows that C6 is approximately sp^2 hybridized. In comparison to **10**, there is an increase of the contribution of the s orbitals in hybridization on C6. For this reason the free radical becomes planar, and the C5–C6, C6–C7, and C6–C11 bonds are shortened (Table 2). The natural bond orbital analysis reveals five double bonds in **12**: C3–C4, C5–C6, C7–C8, C1–C9, and C2–O13. It is worth pointing out that single C–C bonds are shorter than ordinary single bonds, whereas double bonds are longer than ordinary C–C and C–O double bonds (Table 2). This is in agreement with an analysis of resonance structures of **12** which shows that **12** can be presented with two major resonance

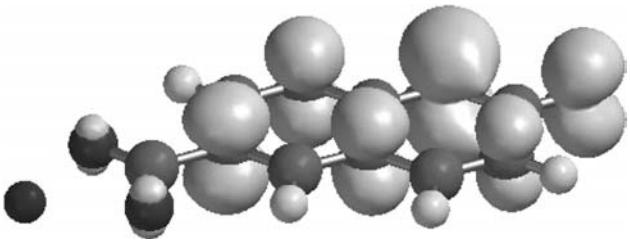

Fig. 3 Spin density surface of the free radical **12**

structures (**12a** and **12b** in Fig. 1). In the resonance structure **12a** the unpaired electron is located on O13, whereas in the resonance structure **12b** the unpaired electron is located on C1. The resonance weightings in the equilibrium geometry of **12** are 30 and 20% for the structures **12a** and **12b**. In addition, the spin density surface of **12** (Fig. 3) shows that the spin density is delocalized over the C1, C3, C6, C8, C10, and O13 atoms. This is in accord with the natural bond orbital analysis which shows that the natural spin density values of the C1, C3, C6, C8, C10, and O13 atoms amount to 0.408, 0.087, 0.159, 0.150, 0.136, and 0.448, whereas the values of all other atoms are very close to zero. On the basis of all these facts it can be concluded, that O13 is the most favorable site of **12** for binding the hydrogen atom. This binding leads to the formation of **13**. A binding of the hydrogen atom to C1 is also plausible, but this binding leads to the formation of a structure whose G^{298} is by 29.9 kJ/mol higher than that of **13**.

Table 1 and Fig. 1 show that the carboxylation reaction of **1** in position 6 is exothermic. Using the free energies, the activation energies for all steps of the reaction are calculated. The activation barriers for the formation of **5** and **9** are relatively low: 52.3 and 49.8 kJ/mol. Higher activation energies are required for the formation of **3** and **7** (114.0 and 139.9 kJ/mol). The rate determining step, *i.e.*, the homolytic cleavage of the C6–H bond requires an expectedly high activation energy of 235.5 kJ/mol. This high activation barrier is in agreement with the experimental conditions for the *Kolbe-Schmitt* reaction [8, 11, 12]. It is also in accord with the values for the energies of activation of similar homolytic cleavages, observed in the carboxylation reactions of alkali metal phenoxides [19].

In comparison to the carboxylation reactions of **1** in positions 1 and 3 [20], the pathway in position 6 is energetically far less favorable. The activation energy for the formation of **3** (Fig. 1) is by 77.6 kJ/mol higher than that for the formation of the corresponding intermediate **3** in Ref. [20]. The energy barrier of the rate determining step (*i.e.*, the formation of **11**) is by 8.2 kJ/mol higher than that for the formation of **7** in Ref. [20]. Finally, G^{298} of **11** is by 47.5 kJ/mol higher than G^{298} of **11** in Ref. [20]. All these findings indicate that (in spite of high temperatures at which the *Kolbe-Schmitt* reaction is performed) **13** will be present in the reaction mixture at very low yield. This is in good accord with the experimental results on the carboxylation reaction of **1** [8, 11, 12].

Methods

To provide the compatibility of the results of this work with the findings of our previous investigation [20], we use the same computational methods. Thus, geometrical parameters of all stationary points and transition states for the carboxylation reaction of **1** in position 6 are optimized in vacuum, at the *B3LYP*/LANL2DZ level of theory [22–24], using the GAUSSIAN98 program package [25]. The vibrational analysis and the natural bond orbital analysis are performed for all structures [26, 27]. All the fully optimized transition state structures are confirmed by the existence of a sole imaginary frequency, whereas the optimized intermediate structures possess only real frequencies. From the transition state structures, the intrinsic reaction coordinates (IRCs) are obtained, and the free energies are maximized along these paths.

Acknowledgements

This work is supported by the Ministry of Science and Environment of Serbia, project No 142025.

References

1. Kolbe H (1860) Liebigs Ann 113:125
2. Schmitt R (1885) J Prakt Chem 31:397
3. Daives IA (1928) Z Phys Chem 134:57
4. Silin NF, Moschtschinkaja NK (1938) J Gen Chem USSR 8:810
5. Gershzon GI (1944) Chem Abstracts 38:1219
6. Chelintsev GV, Smorgonskiĭ LM (1947) Chem Abstracts 41:5466
7. Hales JL, Jones JI, Lindsey AS (1954) J Chem Soc: 3145
8. Lindsey AS, Jeskey H (1957) Chem Rev 57:583
9. Ayres DC (1966) Carbanions in synthesis. Oldbourne Press, London, p 168
10. Kunert M, Dinjus E, Nauck M, Sieler J (1997) Chem Ber/Recueil 130:1461
11. Rahim MA, Matsui Y, Kosugi Y (2002) Bull Chem Soc Jpn 75:619
12. Kosugi Y, Imaoka Y, Gotoh F, Rahim MA, Matsui Y, Sakanishi K (2003) Org Biomol Chem 1:817
13. Marković Z, Engelbrecht JP, Marković S (2002) Z Naturforsch 57a:812

14. Marković Z, Marković S, Begović N (2006) J Chem Inf Model 46:1957
15. Stanescu I, Gupta RR, Achenie LEK (2006) Mol Sim 32:279
16. Stanescu I, Achenie LEK (2006) Chem Eng Sci 61:6199
17. Marković S, Marković Z, Begović N, Manojlović N (2007) Russ J Phys Chem 81:1392
18. Marković Z, Marković S, Manojlović N, Predojević-Simović J (2007) J Chem Inf Model 47:1520
19. Marković Z, Marković S (2008) J Chem Inf Model 48:143
20. Marković Z, Marković S, Đurović I (2008) Monats Chem, published on Web: March 14
21. http://www.ticona.com/redesign/products/vectra_cp
22. Becke AD (1988) Phys Rev A 38:3098
23. Lee C, Yang W, Parr RG (1988) Phys Rev B 37:785
24. Becke AD (1993) J Chem Phys 98:5648
25. Frisch MJ, Trucks GW, Schlegel HB, Scuseria GE, Robb MA, Cheeseman JR, Zakrzewski VG, Montgomery JA Jr, Stratmann RE, Burant JC, Dapprich S, Millam JM, Daniels AD, Kudin KN, Strain MC, Farkas O, Tomasi J, Barone V, Cossi M, Cammi R, Mennucci B, Pomelli C, Adamo C, Clifford S, Ochterski J, Petersson GA, Ayala PY, Cui Q, Morokuma K, Malick AD, Rabuck KD, Raghavachari K, Foresman JB, Cioslowski J, Ortiz JV, Baboul AG, Stefanov BB, Liu G, Liashenko A, Piskorz P, Komaromi I, Gomperts R, Martin RL, Fox DJ, Keith T, Al-Laham MA, Peng CY, Nanayakkara A, Challacombe M, Gill PMW, Johnson B, Chen W, Wong MW, Andres JL, Gonzalez C, Head-Gordon M, Replogle ES, Pople JA (1998) Gaussian 98, Revision A9, Gaussian Inc., Pittsburgh
26. Foster JP, Weinhold F (1980) J Am Chem Soc 102:7211
27. Reed AE, Weinstock RB, Weinhold F (1985) J Chem Phys 83:735